Extent of the annual Gulf of Mexico hypoxic zone influences microbial community structure

Authors:
Lauren Gillies Campbell[1], J. Cameron Thrash[2], Nancy N. Rabalais[3,4], and Olivia U. Mason[1*]

Affiliations:
[1]Department of Earth, Ocean, and Atmospheric Science, Florida State University, Tallahassee, FL 32306, USA
[2]Department of Biological Sciences, Louisiana State University, Baton Rouge, LA, 70803, USA
[3]Department of Oceanography and Coastal Sciences, Louisiana State University, Baton Rouge, LA, 70803, USA
[4]Louisiana Universities Marine Consortium, Cocodrie, LA 70344, USA

Author's emails:
LG Campbell Leg07e@my.fsu.edu, JC Thrash thrash@lsu.edu, NN Rabalais nrabal@lsu.edu, OU Mason omason@fsu.edu

***Corresponding Author**:
Dr. Olivia U. Mason
Email: omason@fsu.edu

Running Title:
Microbes in 2014 nGOM hypoxic zone

Key words:
hypoxia, Gulf of Mexico, iTag, Thaumarchaeota, *amoA*, microbial community structure, ammonia-oxidizing archaea (AOA)

Abstract

Rich geochemical datasets generated over the past 30 years have provided fine-scale resolution on the northern Gulf of Mexico (nGOM) coastal hypoxic (≤ 2 mg of O_2 L^{-1}) zone. In contrast, little is known about microbial community structure and activity in the hypoxic zone despite the implication that microbial respiration is responsible for forming low dissolved oxygen (DO) conditions. Here, we hypothesized that the extent of the hypoxic zone is a driver in determining microbial community structure, and in particular, the abundance of ammonia-oxidizing archaea (AOA). Samples collected across the shelf for two consecutive hypoxic seasons in July 2013 and 2014 were analyzed using 16S rRNA gene sequencing, oligotyping, microbial co-occurrence analysis and quantification of thaumarchaeal 16S rRNA and archaeal ammonia-monooxygenase (*amoA*) genes. In 2014 Thaumarchaeota were enriched and inversely correlated with DO while Cyanobacteria, Acidimicrobiia and Proteobacteria where more abundant in oxic samples compared to hypoxic. Oligotyping analysis of *Nitrosopumilus* 16S rRNA gene sequences revealed that one oligotype was significantly inversely correlated with dissolved oxygen (DO) in both years and that low DO concentrations, and the high Thaumarchaeota abundances, influenced microbial co-occurrence patterns. Taken together, the data demonstrated that the extent of hypoxic conditions could potentially influence patterns in microbial community structure, with two years of data revealing that the annual nGOM hypoxic zone is emerging as a low DO adapted AOA hotspot.

Introduction

Deoxygenation of the ocean is one of the primary consequences of global climate change [1,2], with much attention directed towards coastal hypoxic zones (dissolved oxygen (DO) concentrations below 2 mg L^{-1} or 62.5 µmol/kg). Hypoxic zones are frequently referred to as "dead zones" because they are inhospitable to macrofauna and megafauna; however, microorganisms thrive in such environments [3]. Eutrophication-associated dead zones have been reported in over 500 locations spanning the globe [4] and are predicted to increase in number and size in the near future as a result of increasing greenhouse gas emissions [2]. The northern Gulf of Mexico (nGOM) is the site of the second largest eutrophication-associated coastal dead zone in the world, with bottom water hypoxia extending to over 20,000 km^2 [5] and covering anywhere from 20% to 50% of the water column during the summer months [6]. The nGOM hypoxic zone is influenced by the freshwater input and nutrient load from the Mississippi (MI) and Atchafalaya (AR) Rivers [7], which results in a phytoplankton bloom, the biomass of which is subsequently respired by aerobic microorganisms leading to low DO concentrations or hypoxic zones [8,9]. Hypoxia in the nGOM has increased in severity during the summer months in direct response to additional inorganic nitrogen loading in the Mississippi watershed, beginning around the 1950s, after which the nitrate flux to the nGOM continental shelf tripled [10–12]. Therefore, thermal warming, nutrient rich freshwater discharge and microbial respiration culminate and result in an annually extensive nGOM hypoxic zone, that reached a record size at 8,776 mi^2 (22,720 km^2) in 2017 (LUMCON 2017, https://gulfhypoxia.net/research/shelfwide-cruise/?y=2017, accessed 1/22/2018).

75 While the sequence of events that leads to the nGOM hypoxic zone are well documented [4,13–
76 16], efforts to understand how these chemical, biological, and physical factors influence
77 microbial community structure, abundances, and activity across environmental gradients in the
78 nGOM coastal shelf have only recently been undertaken [17–21]. King and colleagues [17]
79 reported that before the onset of hypoxia (March), Alpha- and Gamma- Proteobacteria,
80 Bacteriodetes and Actinobacteria are abundant in nGOM waters <100m, with Planctomycetes
81 and Verrucomicrobia being less abundant. Gillies and colleagues [20] sampled during the 2013
82 hypoxic event in late July, when hypoxic conditions historically and predictably prevail, and
83 reported that the high normalized abundance of a Thaumarchaeota (100% similar to the
84 ammonia-oxidizing archaea *Nitrosopumilus maritimus* [22]) Operational Taxonomic Unit (OTU)
85 (16S rRNA gene iTag data) and the absolute abundance of Thaumarchaeota 16S rRNA and
86 archaeal *amoA* gene copies (quantitative PCR (qPCR)) were significantly inversely correlated
87 with DO [20]. In this 2013 study, Thaumarchaeota comprised more than 40% of the microbial
88 community (iTag sequence data) in hypoxic samples [20]. In contrast, King and colleagues [17]
89 and Tolar and colleagues [23] showed Thaumarchaeota were present at depths <100m increasing
90 in abundance at depths >100m in the nGOM when conditions are oxic over the shelf. Bristow
91 and colleagues [19] sampled a similar geographic area in 2012 during a historically small
92 hypoxic zone (smallest recorded since 1988) and reported that thaumarchaeal abundances
93 increased with depth; reaching a maximum at 120 m. In their shallow, bottom water (15 m)
94 sample, Thaumarchaeota reached ~15% of the microbial community and the highest rate of
95 ammonia oxidation were reported at this single hypoxic station ([19]; Station 6, see their Fig
96 3A). Further, genomic reconstruction of two *Nitrosopumilus* genomes (79% and 96% complete)
97 assembled from shotgun metagenomic data from a subset of the 2013 hypoxic zone samples

98 [20], combined with complimentary shotgun metatranscriptomic data, revealed that the
99 *Nitrosopumilus* reported in that study were active in the 2013 hypoxic zone (Campbell and
100 Mason, unpublished). Specifically, transcripts from *amoABC* genes, with the same synteny as
101 observed in the genome of *N. maritimus* [24] were identified. These data suggest that
102 nitrification, particularly ammonia oxidation, was actively being carried out in the 2013 hypoxic
103 zone by Thaumarchaeota-- an aerobic process that would continue to draw down oxygen,
104 exacerbating hypoxic conditions across the shallow continental shelf [25,26].
105
106 In the nGOM hypoxic zone, the importance of AOA is only beginning to emerge; however,
107 AOA have been shown to be more abundant than ammonia-oxidizing bacteria (AOB) in
108 terrestrial and marine ecosystems, [27–31], and it is proposed that AOA can outcompete bacteria
109 in low energy conditions [32]. In other oxygen minimum zones (OMZs), several studies have
110 reported an increase in abundance of Thaumarchaeota in low DO samples [18,33–37]. The
111 abundance of archaeal *amoA* transcripts also increases in OMZs [35,36,38].
112
113 Therefore, to begin to fill in the knowledge gaps on microbial community structure and
114 specifically on AOA abundances in the nGOM hypoxic zone, we describe the microbial
115 communities in samples collected in July 2014 within and outside of the 13,080 km^2 hypoxic
116 zone, and compared these to Y14 results to the same thirty-three sites sampled during the Y13
117 hypoxic zone (15,120 km^2) [20]. We expanded sampling in Y14 to include surface water and
118 more bottom water oxygen minimum zone samples, as compared to Y13. Our goal was to
119 determine the influence the extent of the hypoxic zone has on the overall microbial ecology and
120 in particular the abundance of AOA across hypoxic seasons in the nGOM. Further, we sought to

121 determine if the high AOA abundances observed in low DO conditions in this large coastal
122 hypoxic zone occur predictably and, if so, consider the potential ecological implications for an
123 annual increase of AOA in the hypoxic zone.
124

125 Material and Methods

126 Sample collection

127 The 2014 hypoxic zone was mapped over seven days, from 27 July to 2 August 2014 and
128 measured 13,080 km^2. At each of the 52 sites sampled, a sample was collected at the surface
129 (except for sites A'2, B9 and C7) (1 meter below sea level (mbsl); samples designated S for
130 surface; 47 samples total) and near the seafloor at the oxygen minimum zone (19 mbsl avg.
131 collection depth; samples designated B for bottom; 50 samples total). Samples were collected
132 from the surface of the Mississippi River at two sites (0mbsl; designated R2 and R4 for
133 Mississippi River) for a total of ninety-nine samples. For each of the ninety-nine samples
134 collected, temperature, depth, salinity (conductivity) and *in situ* chemistry were determined using
135 a conductivity-temperature-depth (CTD) instrument (SeaBird SBE32 5L bottle carousel).
136 Concentrations of DO, ammonium (NH_4), nitrite (NO_2) + nitrate (NO_3), phosphate (PO_4) and
137 chlorophyll a were determined. The sample location map and subsequent plot of DO data were
138 made with Ocean Data View [39].

139 Oxygen, chlorophyll a and nutrients

140 Oxygen concentrations were determined *in situ* with the CTD dissolved oxygen sensor. Oxygen
141 concentrations were verified using Winkler titrations [40] shipboard. Chlorophyll a samples were
142 concentrated on 25-mm Whatman GF/F filters from 500 ml^{-1} L seawater and stored at -20°C.

Chlorophyll a was extracted using the methods described in the Environmental Protection Agency Method 445.0, "In Vivo Determination of Chlorophyll a in Marine and Freshwater Algae by Fluorescence" [41]; however, no mechanical tissue grinder or HCl were used. Chlorophyll a concentrations were determined using a fluorometer with a chlorophyll a standard (*Anacystis nidulans* chlorophyll a). For nutrients, 60 ml of seawater was filtered through 0.22-µm Sterivex filters into two 30-ml Nalgene bottles and stored at -20°C. Nutrient concentrations were determined by the marine chemistry lab at the University of Washington following the WOCE Hydrographic Program using a Technicon AAII system (http://www.ocean.washington.edu/story/Marine+Chemistry+Laboratory).

Microbial sampling and DNA extractions

From each station, up to 5 L of seawater were collected and filtered with a peristaltic pump both at the surface and at the oxygen minimum. A 2.7-µM Whatman GF/D pre-filter was used and samples were concentrated on 0.22-µM Sterivex filters (EMD Millipore). Sterivex filters were sparged, filled with RNAlater and frozen. Samples were transported to Florida State University on dry ice and stored at -80 until DNA extractions and purifications were carried out. DNA was extracted directly off of the filter by placing half of the Sterivex filter in a Lysing matrix E (LME) glass/zirconia/silica beads Tube (MP Biomedicals, Santa Ana, CA, USA) using the protocol described in [20] which combines phenol:chloroform:isoamyalcohol (25:24:1) and bead beating. Genomic DNA was purified using a QIAGEN (Valencia, CA, USA) AllPrep DNA/RNA Kit and quantified using a Qubit2.0 Fluorometer (Life Technologies, Grand Island, NY, USA).

16S rRNA gene sequencing and analysis

16S rRNA genes were amplified from 10 ng of purified genomic DNA in duplicate using archaeal and bacterial primers 515F and 806R, which target the V4 region of *Escherichia coli* in

accordance with the protocol described in [42,43], used by the Earth Microbiome Project (http://www.earthmicrobiome.org/emp-standard-protocols/16s/), with a slight modification: the annealing temperature was modified to 60 °C. Duplicate PCR reactions were combined and purified using Agencourt AMPure XP PCR Purification beads (Beckman Coulter, Indianapolis, IN) and sequenced using the Illumina MiSeq platform. Ninety-nine samples from 52 stations were sequenced and analyzed. Raw sequences were joined using fastq-join [44] with the *join_paired_ends.py* command and then demultiplexed using *split_libraries_fastq.py* with the default parameters in QIIME version 1.9.1 [45]. Demultiplexed data matching Phi-X reads were removed using the SMALT 0.7.6 akutils phix_filtering with the *smalt map* command [46]. Chimeras were removed using *vsearch –uchime_denovo* with VSEARCH 1.1.1 [47]. Neither PhiX contamination nor chimeric sequences were observed. Sequences were then clustered into operational taxonomic units (OTUs), which was defined as ≥ 97% 16S rRNA gene sequence similarity using SUMACLUST [48]and SortMeRNA [49] with *pick_open_reference.py -m sortmerna_sumaclust*. Greengenes version 13.5 [50] was used for taxonomy. The resulting OTU table was filtered to keep only OTUs that had 10 sequences or more (resulting in 8,959 OTUs), and normalized using cumulative sum scaling (CSS) with metagenomeSeq [51] in R. These sequences will be available in NCBI's SRA and on the Mason server at http://mason.eoas.fsu.edu. While taxonomy was determined using Greengenes, taxonomy for OTUs that were determined to be significantly (Wilcoxon) different between environments (surface and bottom, hypoxic and oxic, Y13 and Y14 samples) were additionally verified beyond the class level using SILVA ACT, version 132 alignment and classification [52] with the confidence threshold set to 70%. To determine close relatives of specific OTUs of interest

NCBI's nucleotide blastn was used to search the Nucleotide collection using Megablast with default parameters [53]. Pairwise sequence comparisons were also carried out using blastn.

Statistics

Multiple rarefactions and subsequently the alpha diversity metrics Shannon (H') [54], observed OTUs (calculates the number of distinct OTUs, or richness) and equitability (Shannon diversity/natural log of species richness; the scale is 0-1.0; with 1.0 indicating that all species are equally abundant) were calculated in QIIME version 1.9.1 using *multiple_rarefactions.py* followed by *alpha_diversity.py*. The Shapiro-Wilk test (*shapiro.test* function) was used to test diversity values and environmental variables for normality in R. In R, the Wilcoxon Rank-Sum test (*wilcox.test* function) with the application of Benjamini-Hochberg's (B-H) False Discovery Rate (FDR) (alpha = 0.05) [55] was used to test for significant differences in diversity values, environmental variables, absolute abundance data (Thaumarchaeota 16S rRNA and *amoA* gene copy numbers per L of seawater) and CSS normalized oligotype data between surface and bottom samples, oxic and hypoxic samples and Y13 and Y14.

Statistically significant differences in all CSS normalized OTU abundances between surface and bottom samples, hypoxic and oxic conditions and between Y13 and Y14 samples were determined using the non-parametric Wilcoxon test in METAGENassist [56], with the B-H correction for multiple tests. Prior to the Wilcoxon test, data filtering was carried out to remove OTUs that had zero abundance in 50% of samples and the interquantile range estimate was used to filter by variance to detect near constant variables throughout [57]. After quality filtering 528 OTUs remained out of 8,960 OTUs for Y14 surface and bottom samples, 623 OTUs remained

out of 7,924 OTUs for Y14 bottom only samples, and 724 OTUs remained out of 9,784 OTUs for the same samples collected in Y13 and Y14.

Beta-diversity of CSS normalized data was examined using non-metric multidimensional (NMDS) scaling with Bray-Curtis in R with the *metaMDS* function in the vegan package [58]. The *envfit* function in vegan was then used to fit vectors of environmental parameters onto the ordinations with p-values derived from 999 permutations with the application of the B-H correction for multiple tests using the *p.adjust* function (we defined corrected p-values ≤ 0.05 as significant). Using the vegan package in RStudio, the non-parametric test adonis [59] was used to test whether microbial community composition was significantly different between clusters of samples (surface and bottom, hypoxic and oxic, year 2013 and 2014, east and west latitudes). The *betadisper* function (vegan) was used to test for homogeneity of multivariate dispersion among sample clusters for surface/bottom samples, hypoxic/oxic samples, Y13/Y14 samples and east/west samples. Betadisper p-values were derived from 999 permutations using the *permutest* function and a B-H correction for multiple tests was performed. Using the psych package [60] in R, the nonparametric Spearman's rank order correlation coefficient (rho (ρ)) and p-values (B-H correction) were determined for environmental variables and CSS normalized OTUs that were significantly different (Wilcoxon) for Y14 surface and bottom samples, hypoxic and oxic samples and Y14 and Y13 same samples.

Co-occurrence analysis between OTUs that were significantly (Wilcoxon) different between Y13 and Y14 was carried out by determining Spearman's correlation coefficients using the psych package in R, similar to [61–64]. Spearman's correlation results were visualized in R for OTUs

that were significantly (corrected p-values ≤ 0.05) correlated with one or more of the three Thaumarchaeota OTUs (4369009, 1584736 and 4073697).

Oligotyping

Shannon entropy (oligotyping) [65,66] analysis was carried out on all 16S rRNA gene sequences identified as *Nitrosopumilus* to identify variability in specific nucleotide positions in this genus. Scripts were used to format QIIME generated data for oligotyping using *q2oligo.py* and *stripMeta.py* [67]. The QIIME command *filter_fasta.py* was used to obtain all *Nitrosopumilus* 16S rRNA gene sequences. All *Nitrosopumilus* 16S rRNA gene data was then analyzed using the oligotyping pipeline version 0.6 for Illumina data [65,66] with the following commands, *o-trim*, *o-pad-with-gaps* and *entropy-analysis*. All oligotype data was CSS normalized using metagenomeSeq in R.

Quantitative PCR

Thaumarchaeal and bacterial 16S rRNA and archaeal *amoA* genes were quantified in duplicate using the quantitative polymerase chain reaction (qPCR) assay. For each qPCR reaction 10 ng of genomic DNA was used. Thaumarchaeota 16S rRNA genes were amplified using 334F and 554R with an annealing temperature of 59°C [68]. Bacterial 16S rRNA genes were amplified using 1369F and 1492R with 56°C as the annealing temperature [68]. Archaeal *amoA* genes were amplified using Arch-*amoA*-for and Arch-*amoA*-rev with 58.5°C as the annealing temperature [29]. Standards (DNA cloned from our samples for Thaumarchaeota 16S rRNA and archaeal *amoA* and *E. coli* for bacterial 16S rRNA) were linearized, purified, and quantified by fluorometry. The reaction efficiencies for the standard curve were calculated from the slope of the curve for all qPCR assays and were 91.1% for Thaumarchaeota 16S rRNA genes, 88.5% for

bacterial 16S rRNA genes and 85.3% for archaeal *amoA* genes. The qPCR data was converted to gene copies L^{-1} of seawater.

Data deposition

All sequences reported in this paper will be deposited into the NCBI sequence archive upon article acceptance to the journal.

Results

In situ chemistry and physical attributes of the 2014 hypoxic zone

All environmental parameters measured, including DO concentrations in all ninety-nine surface and bottom samples and the two surface samples from sites at the MI River mouth (R4 and R2) collected in late July from Y14 are shown in Supplementary Table 1. In Y14, all environmental variables (S1 Table) except chlorophyll a were significant between surface and bottom samples (Wilcoxon with B-H corrected p-values; S2 Table). Average $NO_2 + NO_3$ concentrations were higher in surface samples compared to bottom samples, while NH_4 and PO_4 were higher in bottom samples.

Bottom water hypoxic conditions in 2014 were confined to the coast and shallower depths (S1 Fig), reaching a total area of 13,080 km^2. When looking at bottom samples only, all environmental variables except NH_4, temperature and chlorophyll a were significantly different between hypoxic and oxic samples (S2 Table). Average NO_2+NO_3 and PO_4 concentrations were higher in hypoxic water samples compared to oxic samples, while average salinity

277 concentrations were higher in oxic samples. The average depth of the bottom water hypoxic
278 samples was 15m and the average depth of oxic samples was 25m.

279 ## Microbial community composition across the shelf and with depth
280 ## in the 2014 hypoxic zone

281 ITag sequencing of 16S rRNA genes was used to determine microbial community composition
282 across the shelf in the Y14 nGOM hypoxic zone, surface and bottom samples. This sequencing
283 effort resulted in 11.9 million reads and 8,959 number of OTUs (the full OTU table is included
284 as S3 Table). In the two MI River samples, Actinobacteria, Cyanobacteria and Proteobacteria
285 were the most abundant phyla (Fig 1A) (Thaumarchaeota relative abundances were low, with R4
286 relative abundances being 1.4% and R2 abundances <0.001%). Actinobacteria OTU4345058
287 (ac1) relative abundance was the highest (up to 22% relative abundance at site R4 and 0.7% at
288 the more saline R2 site), decreasing to 0.1% in surface samples near the mouth of the MI River
289 to < 0.001% to undetectable outside of the MI River in surface and bottom samples (avg. in
290 surface samples 3.54×10^{-4} and avg. in bottom samples 3.8×10^{-5}). Cyanobacteria (*Cyanobium*
291 PCC-6307) OTU404788 was the second most abundant OTU in river samples with a higher
292 abundance in the more saline R2 sample (up to 28% at site R2 and 3% at R4). The surface
293 microbial communities had similar dominant phyla to the MI River samples with Cyanobacteria
294 (avg. 33%) and Proteobacteria (avg. 32%), predominantly Gamma- and Alphaproteobacteria
295 being the most abundant, but had lower abundances of Actinobacteria (3%) than in the two river
296 samples (Fig 1A). In surface samples the average relative abundance of Thaumarchaeota, *N.*
297 *maritimus* OTU4369009 was 0.6%.
298
299 **Fig 1. Phyla level bar graph and boxplots of most abundant bacterial and archaeal groups.**

(A) Phyla level bar graph of relativized 16S rRNA gene iTag sequence data, in which only the more abundant bacterial and archaeal groups are shown. Less abundant groups were summed under "Other." Samples are sorted from lowest to highest DO concentrations on the x-axis and surface and bottom samples are differentiated by brackets with the two Mississippi (MI) River samples on the far left. **(B)** Boxplots of most abundant classes for bottom samples plotted along a DO gradient from lowest to highest DO concentrations (* indicates that taxonomy for these phyla were further refined based on the OTU taxonomy in these groups. # indicates that taxonomy was not resolved beyond phylum).

Bottom water (avg. collection depth was 19 m and avg. DO concentration was 2.26 mg L^{-1}) samples were dominated by Proteobacteria (avg. 37%), primarily Gamma- Alpha- and Deltaproteobacteria, as well as Thaumarchaeota (avg. 14%) (Figs 1A and B). The dominant Thaumarchaeota, *N. maritimus* OTU4369009 had an average relative abundance of 13% in bottom water samples. When plotting bottom water data along a DO gradient, several trends emerged. Gammaproteobacteria, Alphaproteobacteria, Bacteroidetes, Cyanobacteria, and the Actinobacteria Acidimicrobiia generally increased in relative abundance with higher DO (Fig 1B). Deltaproteobacteria, MGII Euryarchaeota and Planctomycetes generally increased in abundance with decreasing DO (Fig 1B). In hypoxic samples, Thaumarchaeota were most abundant, particularly at the lowest DO concentration, with decreasing abundances as DO increased (Fig 1B). Of these taxa in the bottom samples, the normalized abundances of Thaumarchaeota and Planctomycetes were significantly inversely correlated with DO (Spearman's ρ for Thaumaechaeota= -0.38 and Planctomycetes= -0.35, corrected p-values $\leq$ 0.05).

Microbial ecology and correlation analyses with environmental variables across the 2014 hypoxic zone

Surface and bottom samples

Statistical analysis of alpha diversity metrics revealed that microbial diversity (Shannon) was significantly lower in the surface samples when compared with bottom samples (Wilcoxon with B-H corrected p-values; S2 Table). Specifically, Shannon diversity indices averaged 5.97 in all nGOM surface samples and 6.02 in the two surface river samples, as compared with 6.45 in bottom samples. Richness (observed species) increased significantly with depth (avg. 329.92 in surface samples and avg. 494.89 in bottom samples). A test of evenness (equitability) between the surface and bottom sample types revealed that surface samples (avg. 0.72) were less even than bottom samples (avg. 0.75).

Non-parametric statistical analysis (Wilcoxon) was then used to determine which OTUs were responsible for the significant difference in species richness when comparing all surface and bottom samples. Seventeen OTUs showed significant differences in their CSS normalized abundances between surface and bottom samples (S2 Fig). Seven of these OTUs had higher average CSS normalized abundances in bottom samples and were significantly inversely correlated with DO (S2 Fig; Spearman's ρ and corrected p-values ≤ 0.05 in S4 and 5 Tables). The dominant Thaumarchaeota, *N. maritimus* OTU4369009 was significantly inversely correlated with DO and positively correlated with $NO_2 + NO_3$ and PO_4 (S4 and 5 Tables).

Bottom water samples

When analyzing bottom water samples alone, Shannon diversity, richness and evenness indices for hypoxic versus oxic samples were not significantly different. However, comparison of the bottom hypoxic and oxic samples, including environmental variables (Wilcoxon), revealed that the CSS normalized abundances of 16 OTUs were significantly different depending on DO status (S3 Fig). Of the 16 OTUs, six had higher CSS normalized abundances in hypoxic samples and were significantly inversely correlated with DO (S3 Fig; Spearman's ρ and corrected p-values ≤ 0.05 in S6 and 7 Tables). Thaumarchaeota, *N. maritimus* OTU4369009 comprised an average of 16% of the microbial community in hypoxic samples, with a peak abundance of 33% of the microbial community in sample A'2 bottom, which had one of the lowest DO concentrations (0.31 mg of O_2 L^{-1}), versus an average of 10% relative abundance in oxic samples. Further, Thaumarchaeota, *N. maritimus* OTU4369009 was significantly inversely correlated with DO in Y14 bottom samples and significantly inversely correlated with NH_4 and temperature in bottom samples (S6 and 7 Tables). Thaumarchaeota, *N. maritimus* OTU4369009 was significantly positively correlated with NO_2+NO_3, PO_4 and salinity in bottom samples (S6 and 7 Tables). While this Thaumarchaeota OTU4369009 was abundant in hypoxic samples and inversely correlated with DO, the normalized abundances were not significantly different between hypoxic and oxic bottom samples (Wilcoxon).

Microbial community organizational structure and drivers in the 2014 hypoxic zone

To examine the primary drivers in structuring the 2014 microbial communities in the surface and in the bottom water nGOM hypoxic zone, whole community 16S rRNA gene sequence data were examined using Bray-Curtis distances with non-metric multidimensional scaling (NMDS). All environmental variables shown as vectors were significantly correlated (corrected p-values ≤

368 0.05) with NMDS axes revealing the primary drivers in influencing the microbial community
369 structure to be DO, depth, NO_2+NO_3, and PO_4 (Fig 2 and S8 Table), with NO_2+NO_3 and PO_4,
370 decreasing with increasing distance from the MI river mouth. While the adonis test for all Y14
371 samples was significant, so too was beta-dispersion, suggesting non homogenous dispersion for
372 these sample clusters.
373
374 **Fig 2. NMDS ordination of normalized 16S rRNA gene iTag sequence data.**
375 **(A)** NMDS ordination of normalized 16S rRNA gene iTag sequence data for all Y14 surface and
376 bottom samples. Mississippi River samples (MI) are in red **(A)**, samples east of the Atchafalaya
377 River (AR) are in magenta and samples west of the AR are in purple. **(B)** NMDS ordination of
378 normalized 16S rRNA gene iTag sequence data of Y14 bottom samples only. Bubble sizes
379 represent DO concentrations e.g. larger bubbles indicate higher DO concentrations. All
380 environmental variables shown as vectors were significantly (corrected p-values ≤ 0.05)
381 correlated with an NMDS axis for both **(A)** and **(B)**.
382
383 To analyze beta diversity in Y14 bottom water hypoxic verses oxic conditions, surface samples
384 were excluded and bottom water samples were examined using NMDS ordination (Fig 2B). An
385 adonis test revealed distinct microbial communities in hypoxic samples as compared to oxic
386 water samples (Fig 2B) (adonis R^2= 0.09 and p-value ≤ 0.05, beta-dispersion F= 0.60 p-value $\geq$
387 0.05). Bottom samples showed significant spatial clustering east and west of the AR (adonis R^2=
388 0.35 and p-value ≤ 0.05, beta-dispersion F= 0.01 p-value ≥ 0.05) (Fig 2B).

389 Taxonomic and functional gene abundances in the 2014 hypoxic
390 zone

Bacterial and thaumarchaeal 16S rRNA and archaeal *amoA* gene copy numbers (qPCR) were determined in surface and bottom water samples. Bacterial 16S rRNA gene copy numbers L^{-1} were similar in the surface (avg. 4.10×10^7) and in the bottom water samples (avg. 3.73×10^7). In contrast, thaumarchaeal 16S rRNA gene copy numbers L^{-1} were significantly higher in bottom water samples (avg. 2.18×10^7) compared to surface samples (avg. 2.19×10^6) as were *amoA* copy numbers L^{-1} (bottom avg. 3.12×10^7 and surface avg. 2.96×10^6) (Wilcoxon, S2 Table). When comparing hypoxic and oxic samples in bottom only samples, thaumarchaeal 16S rRNA gene copy numbers L^{-1} were significantly higher in hypoxic water samples (avg. 3.28×10^7) compared to oxic water samples (avg. 8.87×10^6) as were *amoA* copy numbers L^{-1} (avg. hypoxic 4.65×10^7 and avg. oxic 1.32×10^7) (S2 Table In surface and bottom water samples, and in bottom water only samples, thaumarchaeal 16S rRNA and *amoA* gene copy numbers L^{-1} were significantly positively correlated with each other, NO_2+NO_3 and PO_4 and significantly inversely correlated with DO (S4-7 Tables). The ratio of Thaumarchaeota 16S rRNA:*amoA* gene copy number L^{-1} was one (avg.).

Differences in the extent of hypoxia and microbial community structure between years 2013 and 2014

The total area of low oxygen in Y14 was 13,080 km^2, compared to 15,120 km^2 in Y13 (gulfhypoxia.net). Comparing the same hypoxic sites we sampled in Y13 and Y14 revealed that DO in Y13 samples was lower (avg. 0.62mg/L) than Y14 (avg. 1.1mg/L) and the average depth of the hypoxic zone was deeper in Y13 (17.7m) compared to Y14 (14.6m) (S4 Fig). Ammonium, salinity and temperature were significantly different between the two hypoxic zones (Wilcoxon, S2 Table) with average NH_4 concentrations being higher in Y13. In the Y13 hypoxic

413 zone, the average ammonium and salinity concentrations were higher, while in the Y14 hypoxic
414 zone (which was located at shallower depths) the average temperature was higher.
415
416 Alpha diversity, Shannon, observed (species richness) and equitability were not statistically
417 significantly different between the years. To look at beta diversity between the years, the bottom
418 samples collected at the same stations in Y13 and Y14 were examined using NMDS (S5 Fig),
419 with environmental variables that were significantly correlated with NMDS axes represented as
420 vectors (corrected p-values ≤ 0.05, S8 Table). An adonis test revealed distinct microbial
421 communities in Y14 samples as compared to Y13 samples (S5A Fig) (adonis $R^2= 0.20$ and p-
422 value ≤ 0.05, beta-dispersion $F= 1.07$ p-value ≥ 0.05). Whereas Y14 showed distinct east and
423 west clusters, Y13 did not (adonis $R^2= 0.09$ and p-value ≤ 0.05, beta-dispersion $F= 10.47$ p-value
424 ≤ 0.05) (S5A Fig).
425
426 Analysis of normalized iTag sequence data of bottom samples collected at the same stations in
427 Y13 and Y14 revealed that the phyla Thaumarchaeota, Actinobacteria, Planctomycetes,
428 Euryarchaeota and SAR406 were greater in Y13 than Y14, whereas Cyanobacteria,
429 Proteobacteria and Bacteroidetes were greater in Y14. At the OTU level, 17 had significant
430 normalized abundances between Y13 and Y14 (Wilcoxon). Five of the 17 OTUs were more
431 abundant in Y14, whereas 12 OTUs were more abundant in Y13 (S6 Fig). Specifically,
432 Thaumarchaeota, *N. maritimus* OTU4369009 (S6 Fig), a Thaumarchaeota OTU4073697 (95%
433 similar to cultured representative *Nitrosopelagicus brevis* strain CN25) and Euryarchaeota, MGII
434 OTU3134564 had higher normalized abundances in Y13 than in Y14. Of the five OTUs that had
435 higher abundances in Y14, one was a Thaumarchaeota OTU1584736 (95% similar to cultured

representative *Nitrosopelagicus brevis* strain CN25). The two Thaumarchaeota that were 95% similar to *Nitrosopelagicus brevis* strain CN25 had a one nucleotide (nt) base pair differentiation at 82/250 (G-A) in the 16S rRNA gene sequence.

When comparing absolute abundance data in the same hypoxic sites sampled in both years, thaumarchaeal 16S rRNA and archaeal *amoA* gene copy numbers (qPCR) per L averages were significantly higher (S4 Fig and S2 Table) in Y14 (avg. 3.31×10^7 and 4.52×10^7) than in Y13 (avg. 7.25×10^6 and 6.87×10^6). In both years, copy number per L of each gene was significantly inversely correlated with DO (Spearman's ρ and corrected p-values in S9-12 Tables).

Shannon entropy analysis of Nitrosopumilus 16S rRNA gene sequence data in the 2013 and 2014 hypoxic zones

Due to the high abundances of *Nitrosopumilus* in hypoxic samples in Y13 and Y14, oligotyping analysis was carried out to examine closely related *Nitrosopumilus* (all sequences annotated as such) in relationship to environmental variables. The Y13 iTag data were not analyzed in this way in our previous paper [20], so here we present CSS normalized OTU data oligotyping results for both Y13 and Y14 in the same station samples (n = 35/year). The normalized abundance of oligotype G (G in nt position 115/250) was significantly higher in abundance in hypoxic samples and more abundant in Y13 compared to Y14 (Wilcoxon, S2 Table). Oligotype G was significantly inversely correlated with DO in both Y13 and Y14 (S9-12 Tables). Conversely, oligotype A (A in nt position 115/250) was lower in hypoxic samples in both years (Fig 3). Oligotypes T or C at nt position 115/250 were lower, reaching maximal abundances of 6.45% and 0.29%, respectively.

459 **Fig 3. Ocean Data View plots of DO and *Nitrosopumilus* G oligotype data.**

460 Plots of **(A)** DO concentrations for the same samples collected in Y13 **(B)** and Y14. **(C)**

461 Oligotype data for *Nitrosopumilus* G oligotype for the same samples collected in Y13 (**C**) and

462 Y14 **(D)**.

463

464 # Thaumarchaeota AOA microbial species co-occurrence patterns in

465 # the 2013 and 2014 hypoxic zones

466 Similar to oligotyping analysis, species co-occurrence was not considered in our Y13 dataset.

467 We therefore evaluated species co-occurrences by determining Spearman's correlation

468 coefficients for the same Y13 and Y14 bottom water sites (n = 35/year). For this analysis, we

469 included only the 17 OTUs discussed above that were significantly different between the years

470 (Wilcoxon), which included the three Thaumarchaeota OTUs; 4369009, 1584736, 4073697 (S6

471 Fig). Of the 17 OTUs that were significantly different between Y13 and Y14 same station

472 samples, ten OTUs were significantly correlated at least once with one of the three

473 Thaumarchaeota OTUs in Y13 and/or Y14 hypoxic or oxic samples (Fig 4).

474

475 **Fig 4. Plots representing co-occurrence (Spearman's ρ) data for OTUs of interest.**

476 Co-occurrence (Spearman's ρ) of Thaumarchaeota (*N. maritimus* OTU4369009, *Ca.*

477 *Nitrosopelagicus* OTU1584736 and *Ca. Nitrosopelagicus* OTU4073697) and ten OTUs whose -

478 normalized abundances were significantly different between years (Wilcoxon test with B-H

479 corrected p-values) in the same Y13 and Y14 bottom water samples. Correlations that were

480 significant (corrected p-values ≤ 0.05) are indicated by an *.

481

Discussion

The Y14 hypoxic zone was slightly smaller in size (13,080 km^2), closer to shore and discontinuous as compared to the Y13 hypoxic zone (15,120 km^2) (S4 Fig). In July 2014, wind speeds reached between 10 to 20 knots blowing from the west, with higher than average wave height (1.4 meters) reported (http://www.wavcis.lsu.edu/). Further, in Y14 there was an unseasonably late (late July), above average Mississippi River discharge (avg. is ~ 4 x 10^5 ft^2/sec compared to 5 x 10^5 ft^2/sec in Y14), which resulted in nitrogen ($NO_2 + NO_3$) concentrations reaching a near-record high (200 μmol L^{-1}) and an anomalously high phytoplankton biomass (e.g., 118 ug/L Chl *a* at the end of July) (LUMCON 2014, http://bit.ly/2wHLSk1, accessed 02/08/17) late in the hypoxic season (S1 Table and S1 Fig). These factors could have resulted in the slight DO replenishment seen between 92° W and 92.38° W, specifically along transect G, west of the Atchafalaya River (AR) (S1 Table and S1 Fig). Previous reports of wind out of the west and southwest during the summer months have correlated with a smaller hypoxic zone, which moves nutrient enhanced water masses to the east and to deeper waters, disrupting density stratification [69,70]. Therefore, a plausible hypothesis is that the variability in wind forcing resulted in the movement of water masses to the east [71]. This wind forcing could have influenced the hypoxic area to the west of the Atchafalaya River, resulting in the variability in the size and shape of the hypoxic zone between Y13 and Y14, while also potentially shaping the microbial community as seen in the east west latitude clustering in Y14, but not in Y13 (S4 and 5 Figs).

Specifically, our data revealed a significant inverse correlation between AOA and DO in the nGOM. However, in Y14 when the hypoxic zone was less extensive, and focused at the MI

505 River mouth the normalized abundances of AOA were lower than in Y13. In Y14, although
506 AOA were enriched in the hypoxic bottom water, after correcting for multiple comparisons, their
507 normalized abundances (iTag) were not significantly higher in hypoxic verses oxic samples. Yet
508 the absolute abundances of thaumarchaeal 16S rRNA and *amoA* genes were significantly higher
509 in Y14 than in Y13 (S4 Fig). This discrepancy between iTag and qPCR suggested that the iTag
510 primers did not discern the full breadth of Thaumarchaeota diversity in comparison to qPCR
511 primers. To reconcile the disparity between iTag and qPCR, samples that had high
512 Thaumarchaeota 16S rRNA and *amoA* gene copy number were further analyzed. Both MI River
513 samples had low normalized abundances of Thaumarchaeota (less than 1%), but up to 10^5 copies
514 of Thaumarchaeota 16S rRNA genes/L and 10^6 copies of *amoA* genes/L. These results could be
515 indicative of Thaumarchaeota that are introduced to the nGOM during freshwater input,
516 compared to Thaumarchaeota that are adapted to saline conditions introduced to the hypoxic
517 zone via nGOM seawater in the bottom layer. Therefore, the location and physical parameters of
518 the hypoxic zone could influence Thaumarchaeota abundance and subsequently overall microbial
519 diversity.
520
521 Further comparison of Y13 and Y14 revealed that the *Nitrosopumilus* oligotype G was both
522 annually abundant in the nGOM and was significantly inversely correlated with DO (Fig 3).
523 This oligotype was differentiated by 1 bp in all 16S rRNA gene sequences annotated as
524 *Nitrosopumilus*. Whether this polymorphism is ubiquitous in low DO adapted Thaumarchaeota
525 is not yet known. The data did suggest that its abundance was influenced by the severity of
526 bottom water hypoxia (expansive and deeper verses shallow and smaller), where abundances
527 were greater in Y13 (Fig 3). Thus, this *Nitrosopumilus* oligotype may be adapted to low oxygen,

528 coastal conditions. Oligotyping has revealed ecologically important sub-OTUs in human and
529 environmental microbiomes across environmental gradients [66,72–75]. For example, Sintes and
530 colleagues [74] identified two groups of *amoA* oligotypes that clustered according to high or low
531 latitude and subclustered by ocean depth, however little other oligotypic analysis has been
532 carried out on AOA, specifically *Nitrosopumilus*. Thus, oligotyping can reveal subtle nucleotide
533 variations within AOA. Whether a low DO adapted AOA oligotype that was dominant in coastal
534 hypoxic samples are ecologically consequential remains to be determined.
535
536 Microbial species co-occurrences relationships can reveal community patterns, and facilitate
537 hypothesis generation regarding abiotic influences on random and non-random patterns [61–64].
538 In our study, co-occurrence analysis of OTUs that were significantly different between bottom
539 water sites in Y13 and Y14 revealed that increasing normalized abundances of *N. maritimus*
540 OTU4369009, particularly in Y13, potentially perturbed co-occurrence relationships with other
541 OTUs, specifically MGII Euryarchaeota OTU3134564 and Deltaproteobacteria OTU837775
542 (putatively identified as a SAR324 by SILVA) (Fig 4). Previous studies reported that MGII have
543 an aerobic photoheterotrophic lifestyle [76–78] with higher abundances in the euphotic zone
544 compared to depths below the euphotic zone [28,79–81]. Whereas Thaumarchaeota, closely
545 related to the *N. maritimus*, increase in abundance with depth [17,18,28,79,82]. Therefore, if
546 high thaumarchaeal abundances in the hypoxic zone are not met with higher MGII abundances,
547 potential metabolic linkages would be decoupled, which could be ecologically significant. It has
548 been reported that some SAR324 have the ability to oxidize hydrogen sulfide [83] which could,
549 in theory, mean that when hypoxic conditions prevail and AOA continues to draw down DO,
550 SAR324 could oxidize sulfide that may flux from the sediments resulting in detoxification of

551 bottom water. During hypoxic conditions when *N. maritimus* OTU4369009 abundances are high,
552 co-occurrence with SAR324 abundances are weakened (Fig 4) and sulfide oxidation by SAR324
553 may not keep pace, resulting in a deteriorating environment beyond low DO.
554
555 The two Thaumarchaeota (OTU1584736 and OTU4073697) that were significantly different
556 between the years were significantly positively correlated with each other in both hypoxic and
557 oxic samples in both years (Fig 4). These two OTUs are 95% similar to the *N. Brevis* CN25 [84],
558 an AOA that has been shown to produce N_2O enrichment cultures [85], similar to *N. maritimus*
559 [86,87]. AOA have been reported to be the primary source of N_2O in the surface ocean [85] and
560 it has been shown that decreasing oxygen concentration could influence the production of N_2O
561 by AOA [85,86,88–90]. In the shallow nGOM water column, Walker JT and colleagues [91]
562 reported that nitrification was the primary source of N_2O during peak hurricane season,
563 consistent with the results of Pakulski (2000) [25]. Therefore, the three Thaumarchaeota OTUs
564 that we show to be abundant in the n GOM hypoxic zone of both years may contribute to N_2O
565 production, a potent greenhouse gas [92,93], which can flux from ocean to the atmosphere when
566 the water column is mixed by tropical storm activity [91].
567
568 Additionally, a decoupling between the two-step transformation of ammonium to nitrate (which
569 are carried out by distinct groups of microorganisms) has previously been reported (e.g. [94,95],
570 including in the nGOM hypoxic zone [19]. In our dataset nitrate oxidizing bacteria (NOB) were
571 undetectable, thus the annual increase in AOA in the nGOM, and the lack of co-occurrence with
572 NOB suggested that nitrite may accumulate, as shown by Bristow and colleagues [19] in this
573 expansive hypoxic zone. This metabolic decoupling, leading to NO_2 accumulation during the

574 summer months when the nGOM hypoxic zone develops, is consequential given the toxicity of
575 nitrite [96].
576

577 Conclusion

578 Collectively, this dataset supports that the nGOM hypoxic zone can serve as a hotspot for AOA
579 and the that the normalized abundance of Thaumarchaeota 16S rRNA (iTag) and the absolute
580 abundance (qPCR) of Thaumarchaeota 16S rRNA and archaeal *amoA* gene copy numbers can
581 reflect the extent of bottom water hypoxia. There are few reports describing abundant
582 Thaumarchaeota in shallow coastal environments; most of which represent polar environments
583 [97–101]. Our findings of an increase in Thaumarchaeota in the hypoxic nGOM are consistent
584 with several studies that have reported an increase in abundance of Thaumarchaeota in low
585 oxygen marine environments [18–20,33–36], however this is first known dataset that has
586 sampled the water column microbial community of the shelfwide nGOM hypoxic zone in two
587 consecutive years. Future studies that determine the ecological implications of an AOA hotspot,
588 their co-occurrences and the potential impact on biogeochemical cycling, such as the
589 contribution to N_2O production and their role in ocean deoxygenation, which is intensifying in a
590 changing climate [1,2,102–104] are needed.
591

592 References

593 1. Levin LA, Breitburg DL. Linking coasts and seas to address ocean deoxygenation. Nat
594 Clim Chang. 2015;5(5):401–3.
595 2. Breitburg D, Levin LA, Oschlies A, Grégoire M, Chavez FP, Conley DJ, et al. Declining

oxygen in the global ocean and coastal waters. Science. 2018 Jan 5;359(6371):eaam7240.

3. Wright JJ, Konwar KM, Hallam SJ. Microbial ecology of expanding oxygen minimum zones. Nat Rev Microbiol. 2012 Jul;10(6):381–94.

4. Diaz RJ, Rosenberg R. Spreading dead zones and consequences for marine ecosystems. Science. 2008 Aug 15;321(5891):926–9.

5. Rabalais NN, Turner RE, Wiseman WJ. Gulf of Mexico Hypoxia, A.K.A. "The Dead Zone." Annu Rev Ecol Syst. 2002 Nov;33(1):235–63.

6. Rabalais NN, Turner RE, Wiseman WJ. Hypoxia in the Gulf of Mexico. J Environ Qual. 2001;30(2):320.

7. Rabalais NN, Turner RE. Oxygen depletion in the Gulf of Mexico adjacent to the Mississippi River. In: Neretin LN, editor. Past and present water column anoxia. Springer Netherlands; 2006. p. 225–45.

8. Dagg M, Sato R, Liu H, Bianchi TS, Green R, Powell R. Microbial food web contributions to bottom water hypoxia in the northern Gulf of Mexico. Cont Shelf Res. 2008;28(9):1127–37.

9. Dagg MJ, Ammerman JW, Amon RMW, Gardner WS, Green RE, Lohrenz SE. A review of water column processes influencing hypoxia in the northern Gulf of Mexico. Estuaries and Coasts. 2007 Oct;30(5):735–52.

10. Rabalais NN, Turner RE, Wiseman William J J. Characterization and long-term trends of hypoxia in the northern Gulf of Mexico: Does the science support the Action Plan? Estuaries and Coasts. 2007;30(5):753–72.

11. Chen N, Bianchi TS, McKee BA, Bland JM. Historical trends of hypoxia on the Louisiana shelf: application of pigments as biomarkers. Org Geochem. 2001 Apr 1;32(4):543–61.

12. Rabalais NN, Turner RE, Scavia D. Beyond Science into Policy: Gulf of Mexico Hypoxia and the Mississippi River. Bioscience. 2002;52(2):129.

13. Rabalais NN, Turner RE, Dortch Q, Justic D, Bierman VJ, Wiseman WJ. Nutrient-enhanced productivity in the northern Gulf of Mexico: past, present and future. In: Nutrients and Eutrophication in Estuaries and Coastal Waters. Dordrecht: Springer Netherlands; 2002. p. 39–63.

14. Rabalais N, Turner R, Wiseman WJ. Characterization and long-term trends of hypoxia in the northern Gulf of Mexico: Does the science support the Action Plan? Estuaries and Coasts. 2007;30(5):753–72.

15. Turner RE, Rabalais NN, Justic D. Predicting summer hypoxia in the northern Gulf of Mexico: Riverine N, P, and Si loading. Mar Pollut Bull. 2006;52(2):139–48.

16. Wiseman WJ, Rabalais NN, Turner RE, Dinnel SP, MacNaughton A. Seasonal and interannual variability within the Louisiana coastal current: stratification and hypoxia. J Mar Syst. 1997 Aug;12(1–4):237–48.

17. King GM, Smith CB, Tolar B, Hollibaugh JT. Analysis of Composition and Structure of Coastal to Mesopelagic Bacterioplankton Communities in the Northern Gulf of Mexico. Front Microbiol. 2013;3:438.

18. Tolar BB, King GM, Hollibaugh JT. An analysis of thaumarchaeota populations from the northern gulf of Mexico. Front Microbiol. 2013 Jan;4:72.

19. Bristow LA, Sarode N, Cartee J, Caro-Quintero A, Thamdrup B, Stewart FJ. Biogeochemical and metagenomic analysis of nitrite accumulation in the Gulf of Mexico hypoxic zone. Limnol Oceanogr. 2015 Sep;60(5):1733–50.

20. Gillies LE, Thrash JC, de Rada S, Rabalais NN, Mason OU. Archaeal enrichment in the

642 hypoxic zone in the northern Gulf of Mexico. Environ Microbiol. 2015;17:10pp.

643 21. Thrash JC, Seitz KW, Baker BJ, Temperton B, Gillies LE, Rabalais NN, et al. Metabolic
644 Roles of Uncultivated Bacterioplankton Lineages in the Northern Gulf of Mexico "Dead
645 Zone";. MBio. 2017 Sep 12;8(5):e01017-17.

646 22. Könneke M, Bernhard AE, de la Torre JR, Walker CB, Waterbury JB, Stahl D a. Isolation
647 of an autotrophic ammonia-oxidizing marine archaeon. Nature. 2005 Sep;437(7058):543–
648 6.

649 23. Tolar BB, King GM, Hollibaugh JT. An Analysis of Thaumarchaeota Populations from
650 the Northern Gulf of Mexico. Front Microbiol. 2013;4:72.

651 24. Walker CB, De La Torre JR, Klotz MG, Urakawa H, Pinel N, Arp DJ, et al.
652 Nitrosopumilus maritimus genome reveals unique mechanisms for nitrification and
653 autotrophy in globally distributed marine crenarchaea. Proc Natl Acad Sci U S A. 2010
654 May 11;107(19):8818-23.

655 25. Pakulski JD, Benner R, Whitledge T, Amon R, Eadie B, Cifuentes L, et al. Microbial
656 Metabolism and Nutrient Cycling in the Mississippi and Atchafalaya River Plumes. Estuar
657 Coast Shelf Sci. 2000 Feb;50(2):173–84.

658 26. Nunnally CC, Quigg A, DiMarco S, Chapman P, Rowe GT. Benthic–pelagic coupling in
659 the Gulf of Mexico hypoxic area: Sedimentary enhancement of hypoxic conditions and
660 near bottom primary production. Cont Shelf Res. 2014;85:143–52.

661 27. Francis CA, Roberts KJ, Beman JM, Santoro AE, Oakley BB. Ubiquity and diversity of
662 ammonia-oxidizing archaea in water columns and sediments of the ocean. Proc Natl Acad
663 Sci. 2005 Oct 11;102(41):14683–8.

664 28. Karner MB, DeLong EF, Karl DM. Archaeal dominance in the mesopelagic zone of the

Pacific Ocean. Nature. 2001 Jan;409(6819):507–10.

29. Wuchter C, Abbas B, Coolen MJL, Herfort L, van Bleijswijk J, Timmers P, et al. Archaeal nitrification in the ocean. Proc Natl Acad Sci U S A. 2006 Aug;103(33):12317–22.

30. Mincer TJ, Church MJ, Taylor LT, Preston C, Karl DM, DeLong EF. Quantitative distribution of presumptive archaeal and bacterial nitrifiers in Monterey Bay and the North Pacific Subtropical Gyre. Environ Microbiol. 2007 May;9(5):1162–75.

31. Church MJ, Wai B, Karl DM, DeLong EF. Abundances of crenarchaeal *amoA* genes and transcripts in the Pacific Ocean. Environ Microbiol. 2010 Mar 1;12(3):679–88.

32. Martens-Habbena W, Berube PM, Urakawa H, de la Torre JR, Stahl D a. Ammonia oxidation kinetics determine niche separation of nitrifying Archaea and Bacteria. Nature. 2009 Oct;461(7266):976–9.

33. Belmar L, Molina V, Ulloa O. Abundance and phylogenetic identity of archaeoplankton in the permanent oxygen minimum zone of the eastern tropical South Pacific. FEMS Microbiol Ecol. 2011 Nov;78(2):314–26.

34. Molina V, Belmar L, Ulloa O. High diversity of ammonia-oxidizing archaea in permanent and seasonal oxygen-deficient waters of the eastern South Pacific. Environ Microbiol. 2010 Sep;12(9):2450–65.

35. Lam P, Jensen MM, Lavik G, McGinnis DF, Müller B, Schubert CJ, et al. Linking crenarchaeal and bacterial nitrification to anammox in the Black Sea. Proc Natl Acad Sci U S A. 2007 Apr;104(17):7104–9.

36. Beman JM, Popp BN, Francis C a. Molecular and biogeochemical evidence for ammonia oxidation by marine Crenarchaeota in the Gulf of California. ISME J. 2008 Apr;2(4):429–41.

688 37. Lam P, Lavik G, Jensen MM, van de Vossenberg J, Schmid M, Woebken D, et al.
689 Revising the nitrogen cycle in the Peruvian oxygen minimum zone. Proc Natl Acad Sci U
690 S A. 2009 Mar 24;106(12):4752–7.
691 38. Stewart FJ, Ulloa O, DeLong EF. Microbial metatranscriptomics in a permanent marine
692 oxygen minimum zone. Environ Microbiol. 2012 Jan;14(1):23–40.
693 39. Schlitzer R. Ocean Data View. http://odv.awi.de. 2013.
694 40. Parsons TR, Maita Y, Lalli CM. A manual of chemical and biological methods for
695 seawater analysis. Pergamon Press; 1984. 173p.
696 41. Arar EJ, Collins GB. In vitro determination of chlorophyll a and pheophytin a in marine
697 and freshwater algae by fluorescence. US Environ Prot Agency Method 4450 Revis 12.
698 1997:1–22.
699 42. Caporaso JG, Lauber CL, Walters WA, Berg-Lyons D, Lozupone CA, Turnbaugh PJ, et
700 al. Global patterns of 16S rRNA diversity at a depth of millions of sequences per sample.
701 Proc Natl Acad Sci U S A. 2011 Mar;108 Suppl:4516–22.
702 43. Caporaso JG, Lauber CL, Walters WA, Berg-Lyons D, Huntley J, Fierer N, et al. Ultra-
703 high-throughput microbial community analysis on the Illumina HiSeq and MiSeq
704 platforms. ISME J. 2012 Aug;6(8):1621–4.
705 44. Erik Aronesty. Command-line tools for processing biological sequencing data. github.
706 2011. p. https://github.com/ExpressionAnalysis/ea-utils.
707 45. Caporaso JG, Bittinger K, Bushman FD, DeSantis TZ, Andersen GL, Knight R. PyNAST:
708 a flexible tool for aligning sequences to a template alignment. Bioinformatics. 2010
709 Jan;26(2):266–7.
710 46. Krohn A. akutils-v1.2: akutils-v1.2: Facilitating analyses of microbial communities

711 through QIIME. 2016.

712 47. Rognes T, Flouri T, Nichols B, Quince C, Mahé F. VSEARCH: a versatile open source
713 tool for metagenomics. PeerJ. 2016 Oct;4:e2584.

714 48. Mercier, C., Boyer, F., Bonin, A., & Coissac E. SUMATRA and SUMACLUST: fast and
715 exact comparison and clustering of sequences. 2013;27–9.

716 49. Kopylova E, Noe L, Touzet H. SortMeRNA: fast and accurate filtering of ribosomal
717 RNAs in metatranscriptomic data. Bioinformatics. 2012 Dec;28(24):3211–7.

718 50. McDonald D, Price MN, Goodrich J, Nawrocki EP, DeSantis TZ, Probst A, et al. An
719 improved Greengenes taxonomy with explicit ranks for ecological and evolutionary
720 analyses of bacteria and archaea. ISME J. 2012 Mar;6(3):610–8.

721 51. Paulson JN, Stine OC, Bravo HC, Pop M. Differential abundance analysis for microbial
722 marker-gene surveys. Nat Meth. 2013 Dec;10(12):1200–2.

723 52. Quast C, Pruesse E, Yilmaz P, Gerken J, Schweer T, Yarza P, et al. The SILVA ribosomal
724 RNA gene database project: improved data processing and web-based tools. Nucleic
725 Acids Res. 2012 Nov 27;41(D1):D590–6.

726 53. Altschul SF, Gish W, Miller W, Myers EW, Lipman DJ. Basic local alignment search
727 tool. J Mol Biol. 1990 Oct 5;215(3):403–10.

728 54. Shannon CE, Weaver W. A mathematical theory of communication. 1949. Urbana, IL:
729 University of Illinois Press. 1963.

730 55. Benjamini Y, Hochberg Y. Controlling the False Discovery Rate: A Practical and
731 Powerful Approach to Multiple Testing. Source J R Stat Soc Ser B. 1995;57(1):289–300.

732 56. Arndt D, Xia J, Liu Y, Zhou Y, Guo AC, Cruz J a, et al. METAGENassist: a
733 comprehensive web server for comparative metagenomics. Nucleic Acids Res. 2012

Jul;40:W88-95.

57. Hackstadt AJ, Hess AM. Filtering for increased power for microarray data analysis. BMC Bioinformatics. 2009 Jan 8;10(1):11.

58. Oksanen J, Blanchet FG, Friendly M, Kindt R, Legendre P, McGlinn D, Minchin PR, O'Hara RB, Simpson GL, Solymos P SMF. Vegan: Community Ecology Package. R package version. 2017.

59. Anderson MJ. A new method for non-parametric multivariate analysis of variance. Austral Ecol. 2001 Feb 1;26(1):32–46.

60. Revelle W. Using the psych package to generate and test structural models. 2018.

61. Barberán A, Bates ST, Casamayor EO, Fierer N. Using network analysis to explore co-occurrence patterns in soil microbial communities. ISME J. 2012 Feb;6(2):343–51.

62. Kittelmann S, Seedorf H, Walters WA, Clemente JC, Knight R, Gordon JI, et al. Simultaneous amplicon sequencing to explore co-occurrence patterns of bacterial, archaeal and eukaryotic microorganisms in rumen microbial communities. PLoS One. 2013;8(2):e47879.

63. Williams RJ, Howe A, Hofmockel KS. Demonstrating microbial co-occurrence pattern analyses within and between ecosystems. Front Microbiol. 2014 Jul 18;5:358.

64. Berry D, Widder S. Deciphering microbial interactions and detecting keystone species with co-occurrence networks. Front Microbiol. 2014 May 20;5:219.

65. Eren a. M, Maignien L, Sul WJ, Murphy LG, Grim SL, Morrison HG, et al. Oligotyping: Differentiating between closely related microbial taxa using 16S rRNA gene data. Methods Ecol Evol. 2013;4(12):1111–9.

66. Eren a M, Borisy GG, Huse SM, Mark Welch JL. Oligotyping analysis of the human oral

757 microbiome. Proc Natl Acad Sci. 2014;111(28):E2875–E2884.

758 67. Meadow J. Convert QIIME files into Oligotyping format. 2014. Available from:
759 https://github.com/jfmeadow/q2oligo.

760 68. Suzuki MT, Taylor LT, DeLong EF. Quantitative analysis of small-subunit rRNA genes in
761 mixed microbial populations via 5'-nuclease assays. Appl Environ Microbiol. 2000
762 Nov;66(11):4605–14.

763 69. Feng Y, DiMarco SF, Jackson GA. Relative role of wind forcing and riverine nutrient
764 input on the extent of hypoxia in the northern Gulf of Mexico. Geophys Res Lett. 2012
765 May;39(9).

766 70. Zhang X, Hetland RD, Marta-Almeida M, DiMarco SF. A numerical investigation of the
767 Mississippi and Atchafalaya freshwater transport, filling and flushing times on the Texas-
768 Louisiana Shelf. J Geophys Res Ocean. 2012 Nov;117(C11).

769 71. Feng Y, Fennel K, Jackson GA, DiMarco SF, Hetland RD. A model study of the response
770 of hypoxia to upwelling-favorable wind on the northern Gulf of Mexico shelf. J Mar Syst.
771 2014 Mar;131:63–73.

772 72. Reveillaud J, Maignien L, Eren MA, Huber JA, Apprill A, Sogin ML, et al. Host-
773 specificity among abundant and rare taxa in the sponge microbiome. ISME J. 2014 Jun
774 9;8(6):1198–209.

775 73. Kleindienst S, Grim S, Sogin M, Bracco A, Crespo-Medina M, Joye SB. Diverse, rare
776 microbial taxa responded to the Deepwater Horizon deep-sea hydrocarbon plume. ISME J.
777 2016 Feb;10(2):400–15.

778 74. Sintes E, De Corte D, Haberleitner E, Herndl GJ. Geographic Distribution of Archaeal
779 Ammonia Oxidizing Ecotypes in the Atlantic Ocean. Front Microbiol. 2016;7:77.

780 75. Schmidt VT, Reveillaud J, Zettler E, Mincer TJ, Murphy L, Amaral-Zettler LA.
781 Oligotyping reveals community level habitat selection within the genus Vibrio. Front
782 Microbiol. 2014 Nov 13;5:563.
783 76. Frigaard N-U, Martinez A, Mincer TJ, DeLong EF. Proteorhodopsin lateral gene transfer
784 between marine planktonic Bacteria and Archaea. Nature. 2006 Feb 16;439(7078):847–
785 50.
786 77. Martin-Cuadrado A-B, Rodriguez-Valera F, Moreira D, Alba JC, Ivars-Mart?nez E, Henn
787 MR, et al. Hindsight in the relative abundance, metabolic potential and genome dynamics
788 of uncultivated marine archaea from comparative metagenomic analyses of bathypelagic
789 plankton of different oceanic regions. ISME J. 2008 Aug 8;2(8):865–86.
790 78. Iverson V, Morris RM, Frazar CD, Berthiaume CT, Morales RL, Armbrust EV.
791 Untangling Genomes from Metagenomes: Revealing an Uncultured Class of Marine
792 Euryarchaeota. Science. 2012;335(6068).
793 79. Massana R, Delong EF, Pedrós-Alió C. A few cosmopolitan phylotypes dominate
794 planktonic archaeal assemblages in widely different oceanic provinces. Appl Environ
795 Microbiol. 2000;66(5):1777–87.
796 80. Delong EF. Oceans of Archaea. ASM News-American Society for Microbiology. 2003
797 Oct 1;69(10):503.
798 81. Liu B, Ye G, Wang F, Bell R, Noakes J, Short T, et al. Community Structure of Archaea
799 in the Water Column above Gas Hydrates in the Gulf of Mexico. Geomicrobiol J. 2009
800 Aug 24;26(6):363–9.
801 82. DeLong EF, Taylor LT, Marsh TL, Preston CM. Visualization and Enumeration of Marine
802 Planktonic Archaea and Bacteria by Using Polyribonucleotide Probes and Fluorescent In

803 Situ Hybridization. 1999;65(12):5554–63.

804 83. Swan BK, Martinez-Garcia M, Preston CM, Sczyrba A, Woyke T, Lamy D, et al.
805 Potential for Chemolithoautotrophy Among Ubiquitous Bacteria Lineages in the Dark
806 Ocean. Science. 2011;333(6047).

807 84. Santoro AE, Dupont CL, Richter RA, Craig MT, Carini P, Mcilvin MR, et al. Genomic
808 and proteomic characterization of "Candidatus Nitrosopelagicus brevis" : An ammonia-
809 oxidizing archaeon from the open ocean. Proc Natl Acad Sci U S A. 2015 Jan
810 27;112(4):1173-8.

811 85. Santoro AE, Buchwald C, McIlvin MR, Casciotti KL. Isotopic Signature of N2O
812 Produced by Marine Ammonia-Oxidizing Archaea. Science. 2011;333(6047).

813 86. Löscher CR, Kock A, Könneke M, Laroche J, Bange HW, Schmitz RA. Production of
814 oceanic nitrous oxide by ammonia-oxidizing archaea. Biogeosciences. 2012;9:2419–29.

815 87. Stieglmeier M, Mooshammer M, Kitzler B, Wanek W, Zechmeister-Boltenstern S, Richter
816 A, et al. Aerobic nitrous oxide production through N-nitrosating hybrid formation in
817 ammonia-oxidizing archaea. ISME J. 2014 May 9;8(5):1135–46.

818 88. Naqvi SW a., Bange HW, Farías L, Monteiro PMS, Scranton MI, Zhang J. Marine
819 hypoxia/anoxia as a source of CH_4 and N_2O. Biogeosciences. 2010 Jul 12;7(7):2159–90.

820 89. Peng X, Fuchsman CA, Jayakumar A, Warner MJ, Devol AH, Ward BB. Revisiting
821 nitrification in the Eastern Tropical South Pacific: A focus on controls. J Geophys Res
822 Ocean. 2016 Mar;121(3):1667–84.

823 90. Qin W, Meinhardt KA, Moffett JW, Devol AH, Virginia Armbrust E, Ingalls AE, et al.
824 Influence of oxygen availability on the activities of ammonia-oxidizing archaea. Environ
825 Microbiol Rep. 2017 Jun 1;9(3):250–6.

826 91. Walker JT, Stow CA, Geron C. Nitrous Oxide Emissions from the Gulf of Mexico
827 Hypoxic Zone. Environ Sci Technol. 2010 Mar;44(5):1617–23.
828 92. Ravishankara AR, Daniel JS, Portmann RW. Nitrous oxide (N2O): the dominant ozone-
829 depleting substance emitted in the 21st century. Science. 2009 Oct 2;326(5949):123–5.
830 93. Stocker BD, Roth R, Joos F, Spahni R, Steinacher M, Zaehle S, et al. Multiple
831 greenhouse-gas feedbacks from the land biosphere under future climate change scenarios.
832 Nat Clim Chang. 2013 Jul 14;3(7):666–72.
833 94. Pitcher A, Villanueva L, Hopmans EC, Schouten S, Reichart G-J, Sinninghe Damsté JS.
834 Niche segregation of ammonia-oxidizing archaea and anammox bacteria in the Arabian
835 Sea oxygen minimum zone. ISME J. 2011 Dec 19;5(12):1896–904.
836 95. Hollibaugh JT, Gifford SM, Moran MA, Ross MJ, Sharma S, Tolar BB. Seasonal
837 variation in the metratranscriptomes of a Thaumarchaeota population from SE USA
838 coastal waters. ISME J. 2014 Mar 17;8(3):685–98.
839 96. Camargo JA, Alonso Á. Ecological and toxicological effects of inorganic nitrogen
840 pollution in aquatic ecosystems: A global assessment. Environ Int. 2006 Aug 1;32(6):831–
841 49.
842 97. Tolar BB, Wallsgrove NJ, Popp BN, Hollibaugh JT. Oxidation of urea-derived nitrogen
843 by thaumarchaeota-dominated marine nitrifying communities. Environ Microbiol.
844 2016;00(October):1–13.
845 98. Alonso-Sáez L, Waller AS, Mende DR, Bakker K, Farnelid H, Yager PL, et al. Role for
846 urea in nitrification by polar marine Archaea. Proc Natl Acad Sci U S A. 2012 Oct
847 30;109(44):17989-94.
848 99. Church MJ, Delong EF, Ducklow HW, Karner MB, Preston CM, Karl DM. Abundance

and distribution of planktonic Archaea and Bacteria in the waters west of the Antarctic Peninsula. 2003;48(5):1893–902.

100. Sollai M, Hopmans EC, Schouten S, Keil RG, Sinninghe Damsté JS. Intact polar lipids of Thaumarchaeota and anammox bacteria as indicators of N cycling in the eastern tropical North Pacific oxygen-deficient zone. Biogeosciences 2015;12:4725–37.

101. Galand PE, Casamayor EO, Kirchman DL, Potvin M, Lovejoy C. Unique archaeal assemblages in the Arctic Ocean unveiled by massively parallel tag sequencing. ISME J. 2009 Jul 26;3(7):860–9.

102. Capone DG, Hutchins DA. Microbial biogeochemistry of coastal upwelling regimes in a changing ocean. Nat Geosci. 2013 Sep;6(9):711–7.

103. Altieri AH, Gedan KB. Climate change and dead zones. Glob Chang Biol [Internet]. 2015 Apr 1;21(4):1395–406.

104. Schmidtko S, Stramma L, Visbeck M. Decline in global oceanic oxygen content during the past five decades. Nature. 2017 Feb 15;542(7641):335–9.

Conflict of Interest Statement

The authors declare no conflict of interest.

Author Contributions

LGC, NNR and JCT collected samples. LGC carried out DNA extractions, library preparation and sequencing and statistical analysis of the data. OUM designed the project and did the bioinformatics. LGC and OUM wrote the manuscript.

Funding

Vessel and logistical support was provided by the National Oceanic and Atmospheric Administration, Center for Sponsored Coastal Ocean Research, award numbers NA09NOS4780204 to Louisiana Universities Marine Consortium, N. N. Rabalais PI, and NA09NOS4780230 to Louisiana State University, R. E. Turner, PI.

Acknowledgements

We thank the science and vessel crews of the R/V *Pelican* and Louisiana Universities Marine Consortium for their valuable shipboard and onshore support.

Supporting Information

S1 Fig. (A) Sample map of the 52 stations sampled during the Y14 nGOM shelfwide cruise, in which bottom water status is indicated (red circles indicates oxic stations while blue circles indicates hypoxic stations). (**B)** DO concentrations from the bottom samples collected.

S2 Fig. (A) NMDS ordination of normalized 16S rRNA gene iTag sequence data for all samples collected in year 2014 grouped by surface and bottom. The seventeen bubble plots represent the same NMDS plot with normalized abundances of the OTUs that were statistically significantly different (Wilcoxon) between surface and bottom samples depicted by bubble size, where larger bubble size represents higher normalized abundances. The symbol * represents OTUs that were statistically significantly inversely correlated with dissolved oxygen (Spearman correlation; B-H corrected p-value ≤ 0.05).

S3 Fig. (A) NMDS ordination of normalized 16S rRNA gene iTag sequence data for the all

894 bottom samples collected in year 2014 where bubble size represents DO concentration. The other
895 sixteen NMDS bubble plots represent the normalized abundances of the OTUs that were
896 statistically significantly different (Wilcoxon) between hypoxic and oxic samples. Larger bubble
897 size represents higher normalized abundances. The symbol * represents OTUs that were
898 statistically significantly inversely correlated with dissolved oxygen while the other OTUs are
899 significantly positively correlated with DO (Spearman correlation; B-H corrected p-value ≤
900 0.05).

901 **S4 Fig.** Plots of DO concentrations, relative abundances of Nitrosopumilus
902 OTU4369009 16S rRNA genes (iTag), Thaumarchaeota 16S rRNA and amoA gene copy
903 number/L (qPCR) for bottom water samples collected at the same sites in Y13 and Y14.

904 **S5 Fig. (A)** NMDS ordination of normalized 16S rRNA gene iTag sequence data for the same
905 samples collected in Y13 and Y14 with environmental variables, qPCR data and oligotype data
906 shown as vectors. All environmental variables represented as vectors on the NMDS were
907 significantly correlated (corrected p-value ≤ 0.05) with an NMDS axis. **(B)** The same NMDS
908 ordination depicting oxygen concentration (DO) as bubble size e.g. larger bubbles indicate
909 higher DO concentrations.

910 **S6 Fig. (A)** NMDS ordination of normalized 16S rRNA gene iTag sequence data for the same
911 samples collected in Y13 and Y14 where bubble size depicts oxygen concentration. The other
912 seventeen NMDS bubble plots represent the normalized abundances of the OTUs that were
913 statistically significantly different (Wilcoxon) between the years where larger bubble size
914 represents higher normalized abundances. The symbol * represents OTUs that were statistically
915 significantly inversely correlated with DO in Y14, and the symbol # represents a significant
916 inverse correlation with DO in Y13 (Spearman correlation; B-H corrected p-value ≤ 0.05).

S1 Table. 2014 nGOM hypoxic zone sample metadata and in situ chemistry.

S2 Table. Wilcoxon B-H corrected p-values for diversity statistics and environmental variables for all datasets.

S3 Table. Operational taxonomic unit (OTU) table for all samples collected in 2014.

S4 Table. P-values (B-H corrected) for Spearman's correlation coefficients for Y14 surface and bottom samples.

S5 Table. Spearman's Correlation coefficients (ρ) for Y14 surface and bottom samples.

S6 Table. P-values (B-H corrected) for Spearman's correlation coefficients for Y14 bottom samples only.

S7 Table. Spearman's Correlation coefficients (ρ) for Y14 bottom samples only.

S8 Table. Envfit B-H corrected p-values for NMDS ordinations.

S9 Table. P-values (B-H corrected) for Spearman's correlation coefficients for Y13 same samples only.

S10 Table. Spearman's Correlation coefficients (ρ) for Y13 same samples only.

S11 Table. P-values (B-H corrected) for Spearman's correlation coefficients for Y14 same samples only.

S12 Table. Spearman's Correlation coefficients (ρ) for Y14 same samples only.

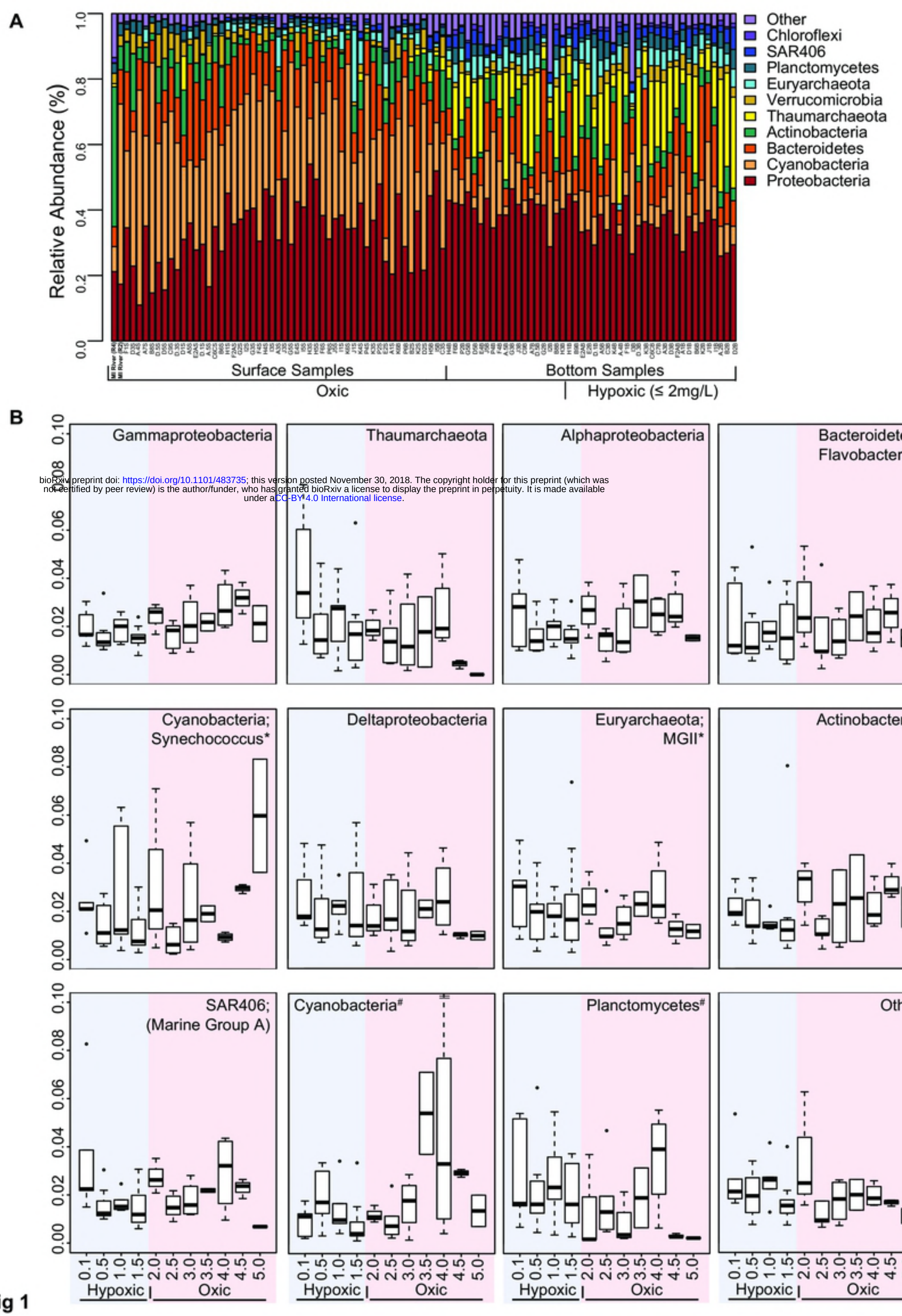

Fig 1

Fig 1

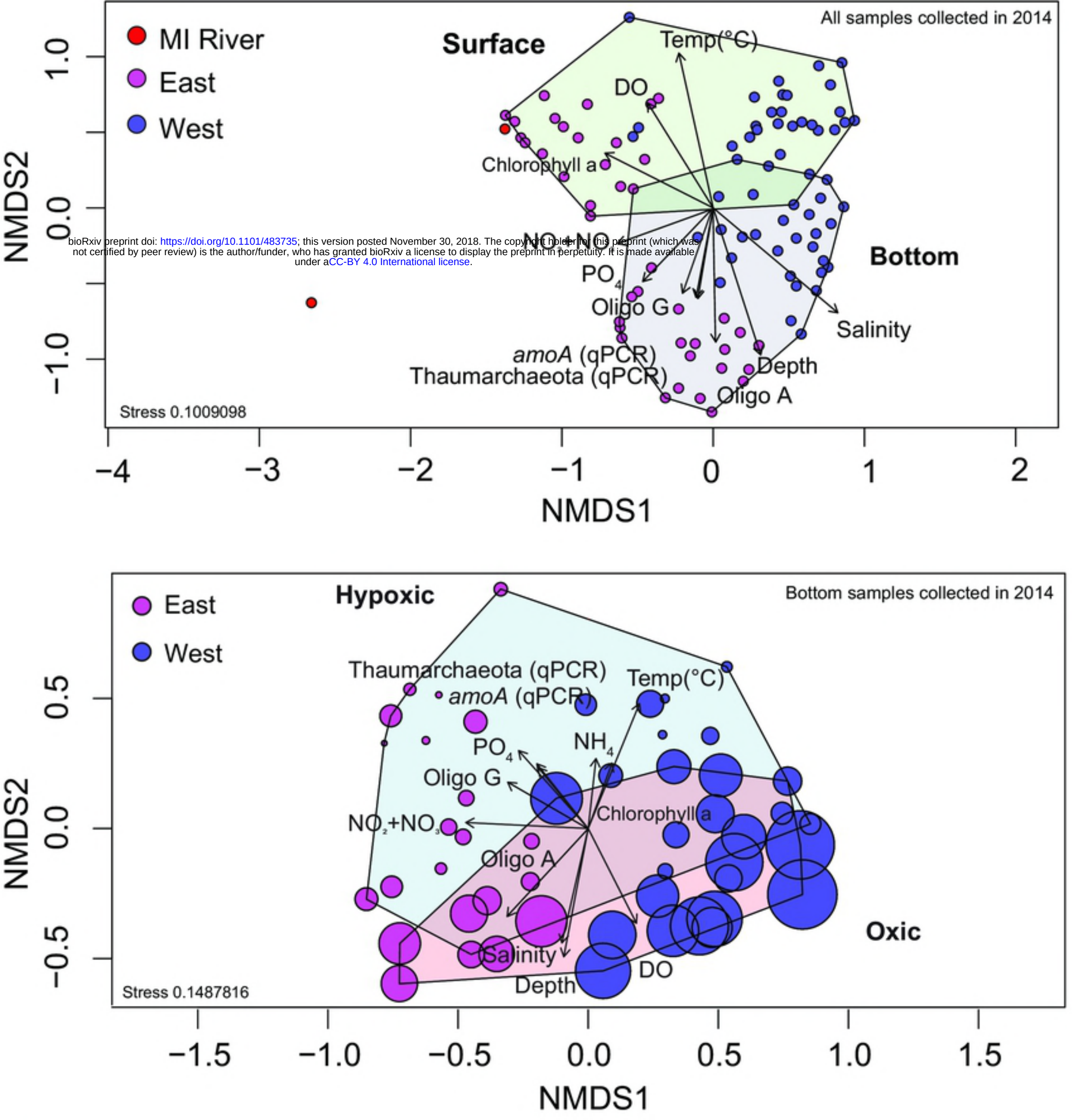

Fig 2

Fig 2

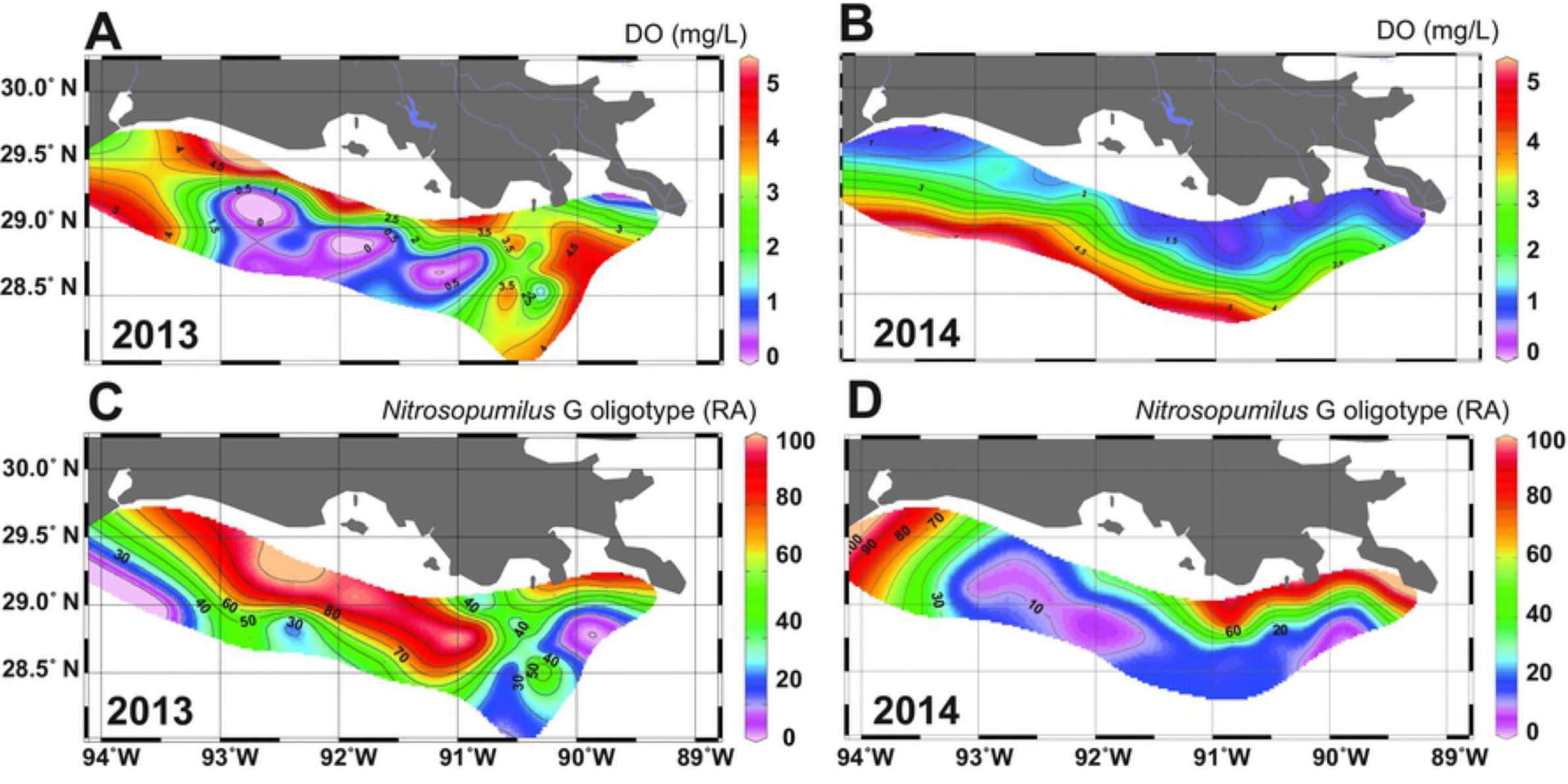
A
DO (mg/L)
30.0° N
29.5° N
29.0° N
28.5° N
2013
5
4
3
2
1
0
B
DO (mg/L)
2014
5
4
3
2
1
0
C
Nitrosopumilus G oligotype (RA)
30.0° N
29.5° N
29.0° N
28.5° N
2013
100
80
60
40
20
0
94°W
93°W
92°W
91°W
90°W
89°W
D
Nitrosopumilus G oligotype (RA)
2014
100
80
60
40
20
0
94°W
93°W
92°W
91°W
90°W
89°W

Fig 3

Fig 3

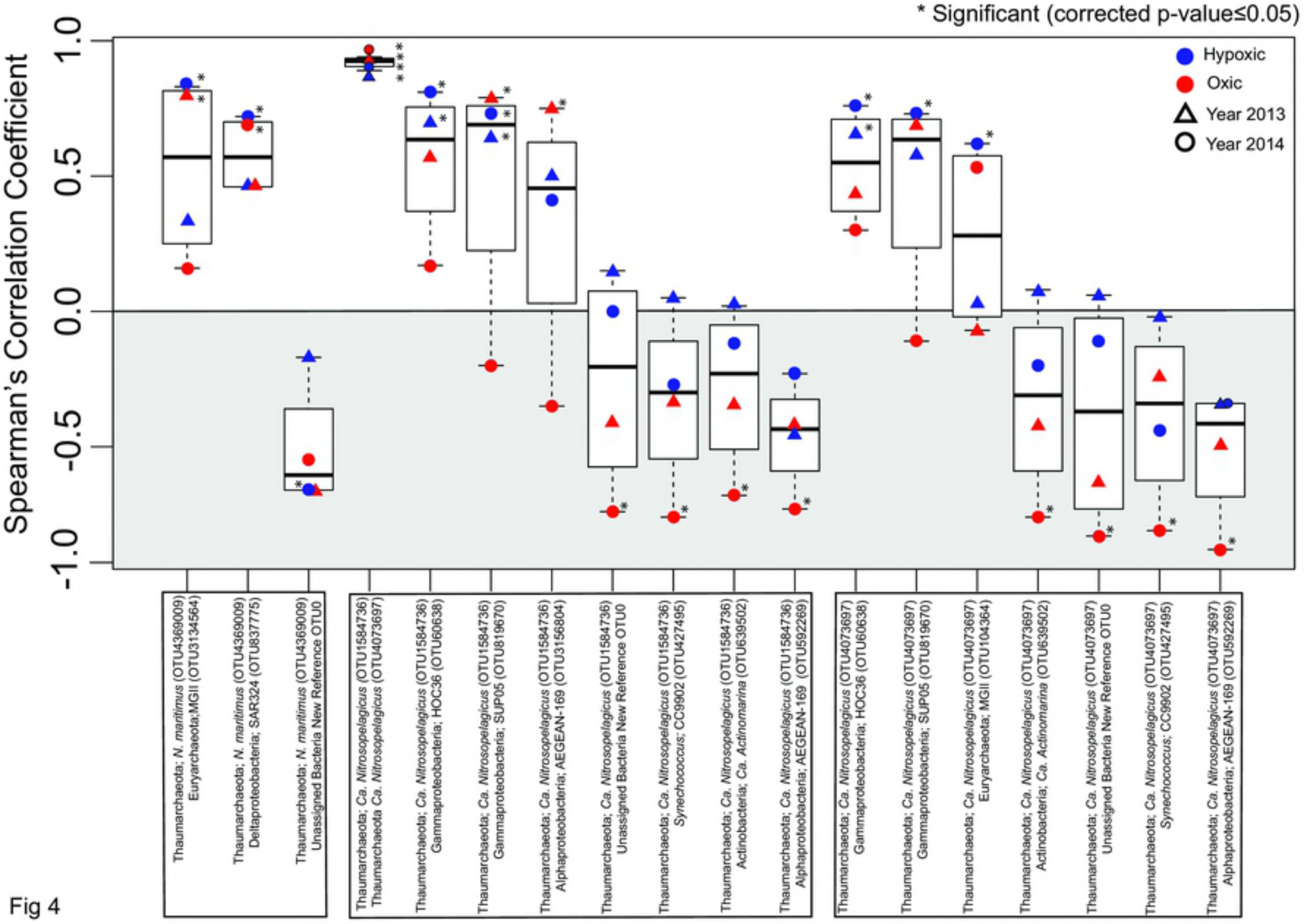
* Significant (corrected p-value≤0.05)
Spearman's Correlation Coefficient
1.0
0.5
0.0
-0.5
-1.0
Hypoxic
Oxic
Year 2013
Year 2014
Thaumarchaeota; N. maritimus (OTU4369009) Euryarchaeota;MGII (OTU3134564)
Thaumarchaeota; N. maritimus (OTU4369009) Deltaproteobacteria; SAR324 (OTU837775)
Thaumarchaeota; N. maritimus (OTU4369009) Unassigned Bacteria New Reference OTU0
Thaumarchaeota; Ca. Nitrosopelagicus (OTU1584736) Thaumarchaeota Ca. Nitrosopelagicus (OTU4073697)
Thaumarchaeota; Ca. Nitrosopelagicus (OTU1584736) Gammaproteobacteria; HOC36 (OTU60638)
Thaumarchaeota; Ca. Nitrosopelagicus (OTU1584736) Gammaproteobacteria; SUP05 (OTU819670)
Thaumarchaeota; Ca. Nitrosopelagicus (OTU1584736) Alphaproteobacteria; AEGEAN-169 (OTU3156804)
Thaumarchaeota; Ca. Nitrosopelagicus (OTU1584736) Unassigned Bacteria New Reference OTU0
Thaumarchaeota; Ca. Nitrosopelagicus (OTU1584736) Synechococcus; CC9902 (OTU427495)
Thaumarchaeota; Ca. Nitrosopelagicus (OTU1584736) Actinobacteria; Ca. Actinomarina (OTU639502)
Thaumarchaeota; Ca. Nitrosopelagicus (OTU1584736) Alphaproteobacteria; AEGEAN-169 (OTU5922269)
Thaumarchaeota; Ca. Nitrosopelagicus (OTU4073697) Gammaproteobacteria; HOC36 (OTU60638)
Thaumarchaeota; Ca. Nitrosopelagicus (OTU4073697) Gammaproteobacteria; SUP05 (OTU819670)
Thaumarchaeota; Ca. Nitrosopelagicus (OTU4073697) Euryarchaeota; MGII (OTU1043641)
Thaumarchaeota; Ca. Nitrosopelagicus (OTU4073697) Actinobacteria; Ca. Actinomarina (OTU639502)
Thaumarchaeota; Ca. Nitrosopelagicus (OTU4073697) Unassigned Bacteria New Reference OTU0
Thaumarchaeota; Ca. Nitrosopelagicus (OTU4073697) Synechococcus; CC9902 (OTU427495)
Thaumarchaeota; Ca. Nitrosopelagicus (OTU4073697) Alphaproteobacteria; AEGEAN-169 (OTU5922269)

Fig 4

Fig 4